Climate Dynamics
https://doi.org/10.1007/s00382-023-07073-2

ORIGINAL ARTICLE

Spatial variability in stable isotopes from Lesotho surface waters: insights into regional moisture transport

Jennifer M. Fitchett[1] · Jonathan A. Holmes[2] · Simoné Dahms-Verster[1] · Christopher J. Curtis[3] · Anson W. Mackay[2]

Received: 1 August 2023 / Accepted: 16 December 2023

Abstract

Precipitation in Lesotho is highly spatially variable, a feature of the high altitude and rugged topography. The hydroclimate dynamics, despite being critical to the water security of Lesotho and adjacent South Africa, are poorly understood. Ratios of oxygen and hydrogen isotopes in meteoric water are excellent tracers of hydroclimatic processes. This study presents the first analysis of stable isotopes from surface waters in Lesotho, and an investigation into the moisture sources. Our results demonstrate considerable variability in isotope values. There are statistically significant relationships between both oxygen and hydrogen isotopes and the altitude of the site and source of rivers sampled, and with hydrogen isotopes and longitude. The meteoric water line for the Lesotho samples is most closely aligned with that of the Global Network of Isotopes in Precipitation (GNIP) station at Harare, in Zimbabwe. The meteoric water line for Windhoek is more closely aligned to the Lesotho samples than the more proximate Cape Town or Pretoria meteoric water lines, which would more closely represent the South African winter- and summer-rainfall zones respectively. HYSPLIT back-trajectory air parcel analysis supports these findings, demonstrating a frequent continental anticyclonic track through southern Zimbabwe. Deuterium excess values vary widely, although are most likely related to processes during moisture transport rather than differences in moisture source. These findings are of particular importance in the context of the future water security of both Lesotho and South Africa, especially as the poleward displacement of the westerly moisture corridor has raised concerns for winter precipitation in the region.

Keywords Precipitation · Stable isotopes · HYSPLIT · Southern Africa · Surface water

1 Introduction

The eastern Lesotho highlands are often referred to as the 'water tower' of southern Africa (UNEP 2010; Hitchcock 2015; Geppert et al. 2022). The hydroclimate of the region is crucial in supplying water to the subsistence farms of Lesotho, and to the economic and industrial hubs of adjacent South Africa through the export of water through the Lesotho Highlands Water Project (Matete and Hassan 2006). While the region currently experiences some of the largest volumes of mean annual precipitation in southern Africa, palaeoclimate records indicate that the eastern Lesotho Highlands have experienced a reduction in surface water availability during the Holocene (Fitchett et al. 2017; Norström et al. 2018). Climate change projections indicate likely reductions in both precipitation and soil moisture for the southern African region under 1.5 – 4 °C warming scenarios to 2080–2100 (Archer et al. 2018; IPCC 2021). For the eastern Lesotho highlands, the projections are less consistent (Morris 2017; Mukwada et al. 2020), but considering both climatic change and future water demand in Lesotho and South Africa through population growth (GCRO 2019), the region is anticipated to face water scarcity before the end of the century, under all modelled climate change scenarios (Pryor et al. 2022). Western Lesotho, which serves as the economic hub of the country, experiences lower total annual rainfall, with dynamics more consistent with those of South Africa (Hydén 2002). The moisture sources of precipitation

✉ Jennifer M. Fitchett
Jennifer.Fitchett@wits.ac.za

1 School of Geography, Archaeology and Environmental Studies, University of the Witwatersrand, Private Bag X3, Wits 2050, South Africa

2 Environmental Change Research Centre, Department of Geography, University College London, Gower Street, London WC1E 6BT, UK

3 Department of Geography, Environmental Management and Energy Studies, University of Johannesburg, Auckland Park, Johannesburg, South Africa

Published online: 01 February 2024

in both eastern and western Lesotho remain poorly understood (Hydén 2002).

Lesotho is located within the summer rainfall zone of southern Africa, with 70–80% of the mean annual precipitation falling between the months of November and March (Sene et al. 1998; Fig. 1). During these months the precipitation comprises orographic rainfall along the escarpment and across the rugged topography (Sene et al. 1998; Xulu et al. 2020), and more short-lived local convection (Dedekind 2015) associated with the Tropical Temperate Trough (TTT) that extends from Namibia to the southeast coast of South Africa (James et al. 2020). Less than 10% of the mean annual precipitation falls during the winter months, predominantly as snowfall, induced by mid-latitude cyclones and associated Cut-off Low (CoL) systems (Stander et al. 2016; Wunderle et al. 2016; Grab et al. 2017). Although a small contribution to the mean annual precipitation, this winter precipitation is likely to diminish with the progressive poleward displacement of the westerlies (Sousa et al. 2018). The TTTs, influenced by ENSO and South Indian Ocean sea surface temperatures (Manhique et al. 2011), are also likely to change in their dynamics under climate change. Key to projecting the hydroclimate future of Lesotho is understanding the moisture transport associated with the synoptic features that drive precipitation in the region, and their relative contributions to seasonal and annual precipitation. The paucity of ground-based meteorological data for Lesotho, and the complexity of the rugged topography present challenges in this regard.

Hydrogen and oxygen Isotope ratios ($^2H/^1H$ and $^{18}O/^{16}O$ respectively) of precipitation and resultant surface waters can serve as important tracers of moisture sources and hydroclimatic processes (Sengupta and Sarkar 2006; Xie et al. 2011; Li et al. 2016; Ren et al. 2017; Geppert et al. 2022). Isotope ratios of oxygen and hydrogen in the water molecule are generally expressed as deviations, in parts per thousand (‰), relative to a standard and expressed in delta (δ) units:

$$\delta(‰) = \left(R_{sample}/R_{standard} - 1\right) \times 1000 \quad (1)$$

Where $R = {}^{18}O/{}^{16}O$ or ${}^2H/{}^1H$ and $\delta = \delta^{18}O$ or δ^2H and the relevant standard for water is VSMOW.

The relationship between δ^2H and $\delta^{18}O$ for meteoric waters worldwide is described by the Global Meteoric Water Line (GMWL), given by:

$$\delta^2H = 8.17 \pm 0.906 \times \delta^{18}O + 10.35 \pm 0.65 \quad (2)$$

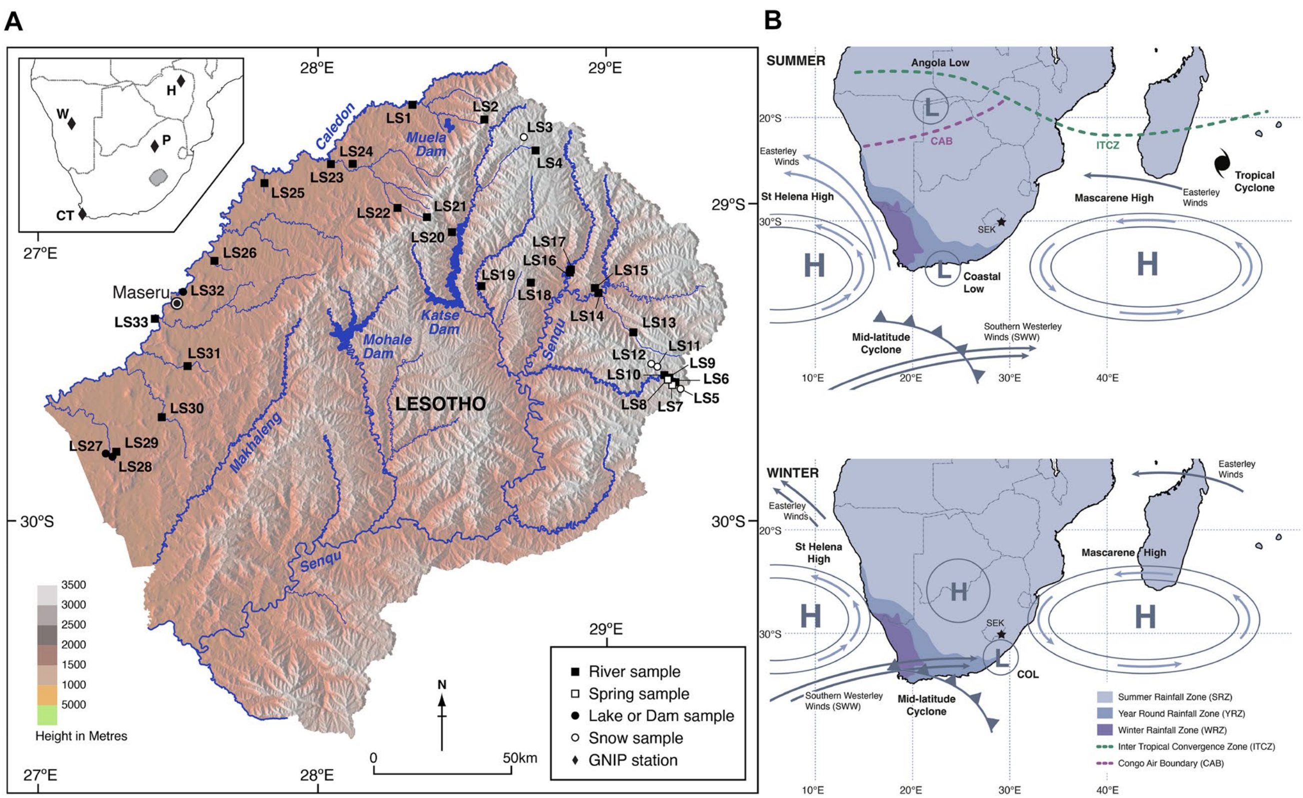

Fig. 1 **A** Topography and major drainage features of Lesotho along with location of the sampling sites for this study. Inset shows location of Lesotho and of the 4 GNIP stations within southern Africa. **B** Major synoptic features of climate over southern Africa. (adapted from Kylander et al. 2021; Saarinen et al. 2022)

Rozanski et al. (1993).

Geographical variations in the δ^2H and $\delta^{18}O$ relationship form Local Meteoric Water Lines (LMWLs), the slope and intercept of which are controlled by moisture source and various atmospheric processes. The intercept of the relationship is referred to as the deuterium excess (d-excess), where:

$$\mathrm{d-excess} \ = \delta^2\mathrm{H} - 8 \ \mathrm{x} \ \delta^{18}\mathrm{O} \tag{3}$$

Dansgaard (1964).

The deuterium excess is a second-order parameter controlled by sea-surface conditions (temperature and especially humidity) at the site of primary evaporation, as well as by the evaporation of raindrops below the cloud base and any addition of 'recycled' moisture to the atmosphere from the land surface (Fröhlich et al. 2002).

Water-isotope data are used extensively to investigate moisture transport ranging from individual rainfall events over very short periods of hours (Soderberg et al. 2013; Good et al. 2014), through to long-term rainfall dynamics over seasons to years (Vystavna et al. 2021; Li et al. 2022a). Many of these studies use data from the International Atomic Energy Agency (IAEA) Global Network of Isotopes in Precipitation (GNIP) in their analyses. While this network comprises more than 1000 sites across 125 countries, it is sparse in southern Africa (Geppert et al. 2022). Only four sites (Cape Town and Pretoria in South Africa, Windhoek in Namibia, and Harare in Zimbabwe; Fig. 1) have long-term records. There are no GNIP stations in Lesotho. A small dataset of surface water analyses from Katse Dame and other unspecified locations in Lesotho is reported as part of the study of de Wet et al. (2020) into the isotopic composition of South African tap water. Analyses of rainwater isotopes from Cape Town (Harris et al. 2010), Mossel Bay (Braun et al. 2017), Thohoyandou (Durowoju et al. 2019) and Johannesburg (Leketa and Abiye 2020), and from sites across Namibia (Kaseke et al. 2016, 2018), confirm the variability in stable isotope ratios across the different rainfall zones that characterise the subcontinent (Geppert et al. 2022), and in turn the value in tracing their moisture sources.

In this study we present a spatial analysis of surface water samples obtained from rivers, dams, springs and snowpack in the northern half of Lesotho in a reconnaissance study, coupled with HYSPLIT moisture back-trajectory modelling. The study has two goals (1) to assess the utility of surface-waters for tracing moisture source and (2) to provide a baseline for future, more detailed, work.

2 Methods

2.1 Study site

Lesotho is a small landlocked country, surrounded entirely by South Africa, spanning 28°34'36.923"S–30°40'56.806"S and 27°0'28.134"E–29°27'47.735"E, covering a land surface area of 30,340km^2 (Mbata 2001; Fig. 1). Lesotho has the highest low point of any country in the world, at 1400 m.asl in the western Lowlands, and a maximum elevation of 3482 m.asl at Thabana Ntlenyana in the eastern Highlands (Grab and Nash 2009). Mean annual precipitation decreases with distance from the Indian Ocean, from approximately 1600 mm in the eastern Highlands along the escarpment (Sene et al. 1998), to 735 mm in the lowlands (Hydén and Sekoli 2000). While the majority of rainfall is experienced during summer months (Sene et al. 1998), snow falls approximately 8 times per annum in the highlands, and once every 2.3 years in the lowlands, predominantly during the colder months of April through September (Grab et al. 2017). Mean annual temperatures range from approximately 6 °C in the highlands to 15 °C in the lowlands, reaching maxima of 29 °C in the lowlands mid-summer, and minima of – 6.1 °C in the highlands in winter (Grab and Nash 2010).

The source of the Senqu-Orange River, the longest and one of the largest rivers in southern Africa, is located in the eastern Lesotho Highlands (Putteman et al. 2011). The Senqu basin, referring to the catchment within the political boundaries of Lesotho, covers approximately two thirds of the land surface area of the country (Pryor et al. 2022). Major tributaries of the Senqu River, including the Mohokare River, flow from the highlands to the lowlands (Chatanga et al. 2019). Despite the uniform basalt geology across the eastern Lesotho Highlands, and sandstone in the western Lesotho Lowlands, the river morphometrics are highly spatially variable (Knight and Grab 2018). Although mean annual precipitation is relatively high, there is only one known natural lake in Lesotho, Letšeng-la Letsie, in the central southern part of the country (Rose et al. 2020). There are, however, a number of small rock-bottom tarns and grass pans in the Sehlabathebe National Park, located along the eastern escarpment (Dunnink et al. 2016). A number of small dams have been built to provide water to cities in the western Lesotho Lowlands (Bates and Haacke 2003; Gwimbi and Selimo 2020). Major dams that were built to form part of the Lesotho Highlands Water Project, which export water to South Africa, include the Katse, Muela and Mohale Dams, while the Polihali Dam which forms part of stage II of the project is still under construction (Tanner et al. 2009; Vinti 2022).

2.2 Field water sampling

Fieldwork was conducted in Lesotho during the winter season between 2 and 5 June 2022. Surface water samples were collected from snowpack, springs, rivers and dams along an approximate E-W transect spanning the eastern Lesotho Highlands and the western Lesotho Lowlands, and a N-S transect along the western border of the country (Fig. 1). Due to the rugged topography and the sparse road network, a convenience sampling approach was used, traversing the major road networks of Lesotho, the majority of which are untarred. Permission for the study was granted by the Lesotho Ministry for Tourism, Environment and Culture.

Water samples for isotope analysis were collected in 50mL polyethylene sample bottles, which were completely filled, sealed and stored in a cool box to prevent evaporation. In the case of snowpack, sample bottles were filled with compacted snow, which later melted out. All samples were later subsampled into 20mL duplicate bottles, and re-sealed for transportation. At each site, GPS coordinates and altitude were recorded using a Garmin eTrex handheld device. For record-keeping, air temperatures were recorded using a Kestrel 5000 handheld device. For samples obtained from rivers, springs and dams, water quality variables including water temperature, pH, electrical conductivity (EC) and dissolved oxygen (DO) were measured using a calibrated YSI multiparameter probe. For the river samples, the river source altitude was obtained from Google Earth, tracing each river to its source, and identifying the altitude from overlaid contours at 20 m intervals (Table 1) following the approach of Lachniet and Patterson (2002).

Water samples were transported to the University College London Bloomsbury Environmental Isotope Facility (BEIF) for analysis. Prior to analysis, aliquots of each sample were filtered and transferred to 2 mL glass Thermo vials. Samples were then analysed for oxygen and hydrogen isotopes by Cavity RingDown Spectroscopy (CRDS) using a Picarro L2130-i analyzer. Results are expressed in δ notation relative to the VSMOW standard. The errors, based on multiple analyses of an in-house standard and the variability on the repeat analyses of the 9 injections for each sample, were better than 0.17 and 1.1‰ for $\delta^{18}O$ and $\delta^{2}H$ respectively.

2.3 Isotopes in southern African precipitation

For evaluation of the surface-waters from Lesotho we used GNIP data from the four southern African stations mentioned previously. For each station, we extracted the weighted mean and annual average $\delta^{18}O$, $\delta^{2}H$ and deuterium excess values as well as the respective local meteoric water lines (LMWLs) determined using penalised weighted least squares regression (PWLSR; Table 1).

Table 1 Details of the four long-term GNIP sites in southern Africa (IAEA/WMO (2023)

GNIP Site	Country	Latitude	Longitude	Altitude (m.asl)	Data range	$\delta^{18}O$ (‰) weighted mean	$\delta^{18}O$ (‰) average	$\delta^{2}H$ (‰) weighted mean	$\delta^{2}H$ (‰) average	d-excess (‰) weighted mean	d-excess (‰) average	Local Meteoric Water Line a	Local Meteoric water Line b	Local Meteoric Water Line r^2
Pretoria	South Africa	−25.73	28.18	1330	1958–1997	−3.85 ± 1.1	−2.68 ± 0.91	−16.8 ± 7.0	−8.8 ± 6.4	14.1 ± 4.3	12.1 ± 4.8	6.81 ± 0.19	9.1 ± 0.87	0.88
Cape Town Airport	South Africa	−33.97	18.6	44	1961–2013	−3.51 ± 0.74	−2.57 ± 0.66	−12.9 ± 4.4	−8.2 ± 3.7	14.1 ± 2.8	11.8 ± 4.0	5.86 ± 0.17	6.74 ± 0.64	0.83
Windhoek	Namibia	−22.95	17.15	1685	1961–2001	−4.99 ± 2.39	−2.59 ± 1.73	−24.3 ± 14.4	−11.3 ± 11.4	12.6 ± 3.7	10.1 ± 3.5	7.30 ± 0.17	9.36 ± 1.0	0.96
Harare	Zimbabwe	−17.83	31.02	1471	1960–2003	−6.18 ± 1.31	−3.78 ± 1.12	−34.3 ± 12.7	−15.9 ± 9.5	13.4 ± 3.1	11.8 ± 3.5	7.87 ± 0.11	12.97 ± 0.72	0.97

Global Network of Isotopes in Precipitation. The GNIP Database. Accessible at: https://nucleus.iaea.org/wiser)

2.3.1 Identifying moisture sources of precipitation in Lesotho

To identify the various moisture sources and air-mass pathways of precipitation in Lesotho, the National Oceanographic and Atmospheric Association (NOAA) Hybrid Single Particle Lagrangian Integrated Trajectory (HYSPLIT) model (Stein et al. 2015) was used. Following the methodology detailed by Li et al. (2022a) for moisture trajectory analysis in alpine river watersheds, back trajectories of all air parcels were modelled in HYSPLIT from the central field-sampling GPS coordinates of 29.11°S, 28.47°E for the 72-hours preceding each day of precipitation at the same coordinates, at 6-hourly resolution, and at three levels of 500 m, 1000 and 2000 m above ground level. Because the isotopic composition of streams and rivers often approximates the mean weighted precipitation isotope value (Mook 2006), we conducted this analysis for each precipitation event in the centre of our sampling region for a full calendar year prior to sampling. As there is a paucity of meteorological data in Lesotho (Sene et al. 1998), rainfall days were estimated using the Climate Hazards Group InfraRed Precipitation with Station (CHIRPS) gridded rainfall data (Funk et al. 2015). Days with snowfall were identified from Snow Report South Africa. Input data for HYSPLIT include cloud height, wind direction, temperature and surface pressure (Bagheri et al. 2019), which were obtained from the Global Data Assimilation System (GDAS) global 1° resolution meteorology data. Dominant air-mass pathways were identified, and their proportional representation calculated, through cluster analysis of all moisture tracks calculated from each of the model runs (Rose et al. 2020; Li et al. 2022a). A second set of HYSPLIT runs were modelled for 72-hour back trajectories of the same set of precipitation dates, with the overlay of relative humidity from the GDAS global 1° database (Rapolaki et al. 2020), to identify those trajectories that had air parcels saturated with moisture along or in the terminal phase of their path.

3 Results

A total of 35 samples were collected from 33 sites (Table 2) including rivers, snowpack (LS3, LS5, LS11, LS12), springs (LS7, LS8) and dams (LS27, LS28, LS32). Snow samples were collected at a maximum altitude of 3205 m. asl (LS3), while river sample sites ranged in altitude from 3063 m. asl (LS4) to 1461 m.asl (LS33; Table 1). River source altitudes ranged from 3350 m.asl (LS14) to 1690 m.asl (LS29; Table 1). For the river samples, DO ranged from 86.6% (7.98 mg/l, LS21) to 127.8% (12.51 mg/l, LS26), while generally higher levels were recorded for the dam samples (Table 2). The EC was generally much lower in the alpine regions, as would be expected for first order streams, increasing in western Lesotho lowlands, with values ranging from 191.1 µS/cm (LS21) to 317.5 µS/cm (LS32, Table 2). The EC for the dams was representative of that of the nearby rivers, and considerably higher than the high-altitude streams (Table 2). Both air and water temperature varied both by altitude and time of day (Table 2).

The isotope values for the dataset as a whole range from + 0.40 to – 18.53‰ and + 1.5 to – 138.3‰ for δ^{18}O and δ^{2}H respectively (Table 3). The lowest δ^{18}O and δ^{2}H values are recorded for the samples from the snowpacks, ranging from – 18.53‰ (LS11-2) to -5.85 (LS3-2) for δ^{18}O: corresponding values for δ^{2}H are – 138.3 (LS12) and – 28.9‰ (LS3-2). This snow remained on the land surface following a snowfall event on 23 May 2022 and there had been no further precipitation events that date until the time of sampling. The d-excess values for snowpack varied from 17.9‰ (LS3-2) to 9.4‰ (LS5).

For the 24 river samples, the mean δ^{18}O is – 3.78‰ ($\sigma = 0.84$‰), with individual values ranging from – 2.29‰ (LS15) to – 2.25‰ (LS21). For δ^{2}H, the mean is -20.0‰ ($\sigma = 4.9$‰) and the individual values range from – 13.8‰ (LS26) to – 2.29.1‰ (LS10). The mean value for d-excess is 10.2‰ ($\sigma = 3.0$‰), with a range of 17.4‰ (LS21)–2.2.9‰ (LS16). Comparing the mean isotope values for samples from the eastern Lesotho Highlands (samples LS2-LS21, > 2000 m.asl) to those from the western Lowlands (samples LS1, LS22-33) using the two-tailed t-test, statistically significant differences are calculated for δ^{18}O ($t = 2.23$, $p = 0.0361$) and δ^{2}H ($t = 3.44$, $p = 0.0023$). For d-excess, the difference in means between samples from the Highlands and Lowlands is not statistically significant ($t = 0.044$, $p = 0.9656$).

The isotopic values for the two samples from springs did not differ markedly from those of the river samples (δ^{18}O values of – 4.11‰ – 4.70‰, δ^{2}H values of – 23.9‰ and – 26.5‰ and d- excess values of 9.2‰ and 11.1‰ were obtained for samples LS-7 and LS-8 respectively) whereas the dam samples show slight heavy-isotope enrichment, with δ^{18}O and δ^{2}H values ranging from + 0.40‰ and + 1.5‰ respectively (LS28) to – 2.76‰ and – 13.6‰ respectively (LS32), with wide variation in d-excess.

The δ^{18}O and δ^{2}H values for all water and snow-pack samples are strongly correlated and described by an ordinary-least squares regression given by:

$$\delta^2\mathrm{H} = 7.8 \text{ x } \delta^{18}\mathrm{O} + 9.9\left(\mathrm{R}^2 = 0.99\right) \tag{4}$$

for the entire dataset excluding the lake samples, which appear to lie on an evaporation line.

Table 2 Location, sample details and physical variables of water samples

Site	Latitude	Longitude	Site Altitude (m.asl)	Source altitude (m.asl)	Air temp (°C)	Water temp (°C)	DO %	DO mg/l	EC µS/cm	pH	Date (2022)	Time	Sample Type
LS1	28°42'29.7"S	28°19'41.9"E	1443	1650	20.8	13.3	110	9.9	233.1	7.81	02/06	14:49	River
LS2	28°55'53.8"S	28°35'00.00"E	2357	2710	19.4	11.1	120.7	10.07	68.3	8.17	02/06	15:26	River
LS3	28°48'52.2"S	28°43'15.9"E	3205	–	10.1	–	–	–	–	–	02/06	16:05	*Snow
LS4	28°51'27.6"S	28°46'13.6"E	3063	3200	10.4	5.6	115.3	10.19	31.9	7.58	02/06	16:26	River
LS5	28°51'37.6"S	28°46'13.6"E	2791	–	2	–	–	–	–	–	03/06	08:50	Snow
LS6	29°35'01.4"S	29°16'08.7"E	2785	2920	7.4	0.8	107.1	11.02	84.3	7.18	03/06	09:24	River
LS7	29°35'07.5"S	29°15'57.5"E	2791	–	7.3	–	–	–	–	–	03/06	09:35	Spring
LS8	29°33'48.7"S	29°14'49.9"E	2744	–	10.2	7.8	113	9.87	98.7	6.82	03/06	10:23	Spring
LS9	29°33'48.3"S	29°14'50.2"E	2712	2920	10.1	4.6	112.9	10.57	87.2	7.09	03/06	10:28	River
LS10	29°33'18.1"S	29°14'05.5"E	2693	3000	14.7	1.3	119.7	12.27	49.6	7.51	03/06	10:44	River
LS11	29°31'36.7"S	29°12'24.1"E	3159	–	5.4	–	–	–	–	–	03/06	10:58	*Snow
LS12	29°31'19.3"S	29°11'26.4"E	3144	–	7.2	–	–	–	–	–	03/06	11:12	Snow
LS13	29°25'22.8"S	29°07'08.1"E	2305	3260	12.7	4.3	102.1	10.18	69.6	7.8	03/06	11:41	River
LS14	29°17'25.0"S	28°59'23.1"E	2006	3350	20.5	5.4	116.9	11.76	91.2	7.78	03/06	12:41	River
LS15	29°17'07.0"S	28°59'02.1"E	2117	2300	19.1	13.5	96.7	8.06	227.5	7.73	03/06	12:55	River
LS16	29°14'15.9"S	28°53'36.6"E	2054	2160	21.2	14	105.4	8.56	244.9	8.05	03/06	13:28	River
LS17	29°14'24.7"S	28°53'31.9"E	2031	3120	18.2	7.9	110.8	10.49	130.9	7.9	03/06	13:40	River
LS18	29°16'40.6"S	28°44'56.6"E	2445	2795	18.4	9.9	114	9.71	148.4	7.82	03/06	14:57	River
LS19	29°16'10.8"S	28°35'08.2"E	2162	3150	17.7	7.5	124.1	11.7	134	7.9	03/06	16:18	River
LS20	29°06'45.6"S	28°28'16.8"E	2150	2650	5.1	4.7	100.6	10.1	100.9	8.26	04/06	08:33	River
LS21	29°04'24.1"S	28°22'54.7"E	2613	2810	3.8	6	86.6	7.98	19.1	8.36	04/06	09:04	River
LS22	29°02'15.0"S	28°16'44.8"E	1829	2660	15.2	5.6	104.1	10.07	102.2	7.38	04/06	09:31	River
LS23	28°53'46.2"S	28°06'51.8"E	1630	1850	18	6.7	120.2	12.28	228.9	7.5	04/06	10:28	River
LS24	28°53'34.4"S	28°02'31.7"E	1559	2070	22	7.5	107.6	10.87	136.1	7.63	04/06	11:12	River
LS25	28°57'18.8"S	27°48'08.3"E	1574	1719	19.6	8.6	107.5	10.53	176.3	7.69	04/06	12:00	River
LS26	29°11'28.6"S	27°37'21.0"E	1531	1730	18.9	8.9	127.8	12.51	246.7	7.78	04/06	12:56	River
LS27	29°48'39.9"S	27°15'00.9"E	1636	–	18.1	12.2	143.3	12.76	253.9	8.16	04/06	15:14	Dam
LS28	29°48'22.1"S	27°14'03.2"E	1641	–	20.7	13.5	100.4	8.77	146.5	7.92	04/06	15:29	Dam
LS29	29°47'51.5"S	27°15'31.4"E	1636	1690	18.2	12.3	127.3	11.33	291.6	7.98	04/06	16:21	River
LS30	29°41'20.0"S	27°26'13.7"E	1552	1820	17.3	13.1	103.6	9.16	219.5	8.02	04/06	16:46	River
LS31	29°31'23.2"S	27°31'19.2"E	1558	1740	11.6	9.7	108.1	10.32	202.2	8.08	04/06	17:10	River
LS32	29°18'00.2"S	27°30'48.4"E	1499	–	7.1	7.2	51.5	5.28	317.5	7.85	05/06	08:30	Dam
LS33	39°22'39.6"S	27°24'33.4"E	1461	2310	12.8	7.4	93.6	9.61	214.7	7.93	05/06	09:47	River

Table 3 Isotope values

Sample Number	Sample Type	$\delta^{18}O$	$\delta^{2}H$	d-excess
LS-1	River	– 3.04	– 15.2	9.2
LS-2	River	– 4.54	– 22.9	13.4
LS-3-1	Snow	– 8.40	– 49.5	17.7
LS-3-2	Snow	– 5.85	– 28.9	17.9
LS-4	River	– 4.64	– 24.0	13.2
LS-5	Snow	– 15.53	– 114.8	9.4
LS-6	River	– 4.97	– 28.1	11.6
LS-7	Spring	– 4.11	– 23.9	9.0
LS-8	Spring	– 4.70	– 26.5	11.1
LS-9	River	– 3.82	– 24.0	6.6
LS-10	River	– 5.02	– 29.1	11.1
LS-11-1	Snow	– 9.67	– 61.4	15.9
LS-11-2	Snow	– 16.75	– 123.3	10.7
LS-12	Snow	– 18.53	– 138.3	9.9
LS-13	River	– 4.84	– 27.8	10.9
LS-14	River	– 4.68	– 26.7	10.8
LS-15	River	– 2.29	– 14.8	3.5
LS-16	River	– 2.37	– 16.1	2.9
LS-17	River	– 3.81	– 22.0	8.5
LS-18	River	– 4.03	– 20.9	11.3
LS-19	River	– 3.64	– 18.3	10.8
LS-20	River	– 3.12	– 15.1	9.9
LS-21	River	– 5.25	– 24.4	17.6
LS-22	River	– 3.33	– 15.8	10.8
LS-23	River	–3.58	– 16.9	11.8
LS-24	River	– 3.74	– 19.1	10.8
LS-25	River	– 3.19	– 14.6	10.9
LS-26	River	– 2.86	– 13.8	9.0
LS-27	Dam	– 2.51	– 12.6	7.5
LS-28	Dam	0.40	1.5	-1.8
LS-29	River	– 3.29	– 17.1	9.2
LS-30	River	– 3.30	– 16.8	9.6
LS-31	River	– 4.15	– 22.4	10.8
LS-32	Dam	– 2.76	– 13.6	8.4
LS-33	River	– 3.10	– 14.8	10.0

Following the analysis of Lachniet and Patterson (2002), the correlations between the isotopic ratios for the river samples against a range of geographical characteristics were calculated using Pearson's correlation coefficient. For both $\delta^{18}O$ and $\delta^{2}H$, statistically significant correlations are calculated for the relationships between isotope values and the altitudes of both the sample site and of the river source (Table 4; Fig. 2 – shown for $\delta^{18}O$ only). The strongest correlation is calculated for $\delta^{2}H$ and site altitude ($r = 0.71$, $p = 0.0001$). Notably, for both $\delta^{18}O$ and $\delta^{2}H$, stronger correlations are calculated for the site altitudes than for the source altitudes of the rivers. For $\delta^{2}H$, a statistically-significant correlation is also calculated between the isotope values and longitude of the site. Given the position of Lesotho, longitude additionally serves as a proxy for distance from the Indian Ocean. No statistically significant correlations are calculated between isotope values and latitude (Table 4). No statistically significant relationships are calculated between d-excess and any of the geographical variables (Table 4). However, d-excess shows variability with $\delta^{18}O$. For the snowpack samples, albeit few in number, there is an increase in d excess with $\delta^{18}O$ whereas for the other samples, d-excess decreases sharply with increase in $\delta^{18}O$ (Fig. 3).

4 Discussion

4.1 Local Meteoric Water Lines

As the slope and y-axis intercept are indicative of moisture source, physical setting and climatic conditions, and because the isotopic composition of surface waters can reflect weighted annual precipitation in some circumstances, local meteoric water lines can be used to investigate the source of surface water. As there are no GNIP stations in Lesotho, there is no published meteoric water line based on precipitation for comparison. We therefore present the local meteoric water line for our samples, and the meteoric water lines for each of the four southern African GNIP stations at Harare, Windhoek, Cape Town and Pretoria (Fig. 4). We note that LMWL from a two-year-long daily rainfall isotope record from Johannesburg (Lakete and Abiye 2020) is very similar to that from the GNIP station at near-by (~60 km) Pretoria, as would be expected. We also note the close similarity between our local meteoric water line for Lesotho and a best-fit line through oxygen and hydrogen isotope values for Lesotho surface waters reported in de Wet et al. (2020; their Fig. 11).

The two GNIP stations closest to Lesotho are Cape Town Airport and Pretoria. Notably, Cape Town is located within the contemporary winter-rainfall-zone of southern Africa, with the westerlies forming the primary moisture source (Roffe et al. 2022). Pretoria and Johannesburg are located within the summer-rainfall-zone, and similar to Lesotho, the majority of rainfall is convective in nature, associated with the TTT (Todd and Washington 1999; Crétat et al. 2012). Based both on proximity and on the synoptic conditions, we would anticipate that the Lesotho MWL would sit between the Pretoria and Cape Town MWLs, likely with a slope more similar to that of Pretoria. However, both the slope and the y-intercept are most similar to the Harare MWL, and are more similar to Windhoek than to either Pretoria or Cape Town (Fig. 4). Notably, even the snow samples, which are from a single, known precipitation event, and which are understood to be a feature of the CoL system associated with the westerlies, predominantly sit on the Harare and

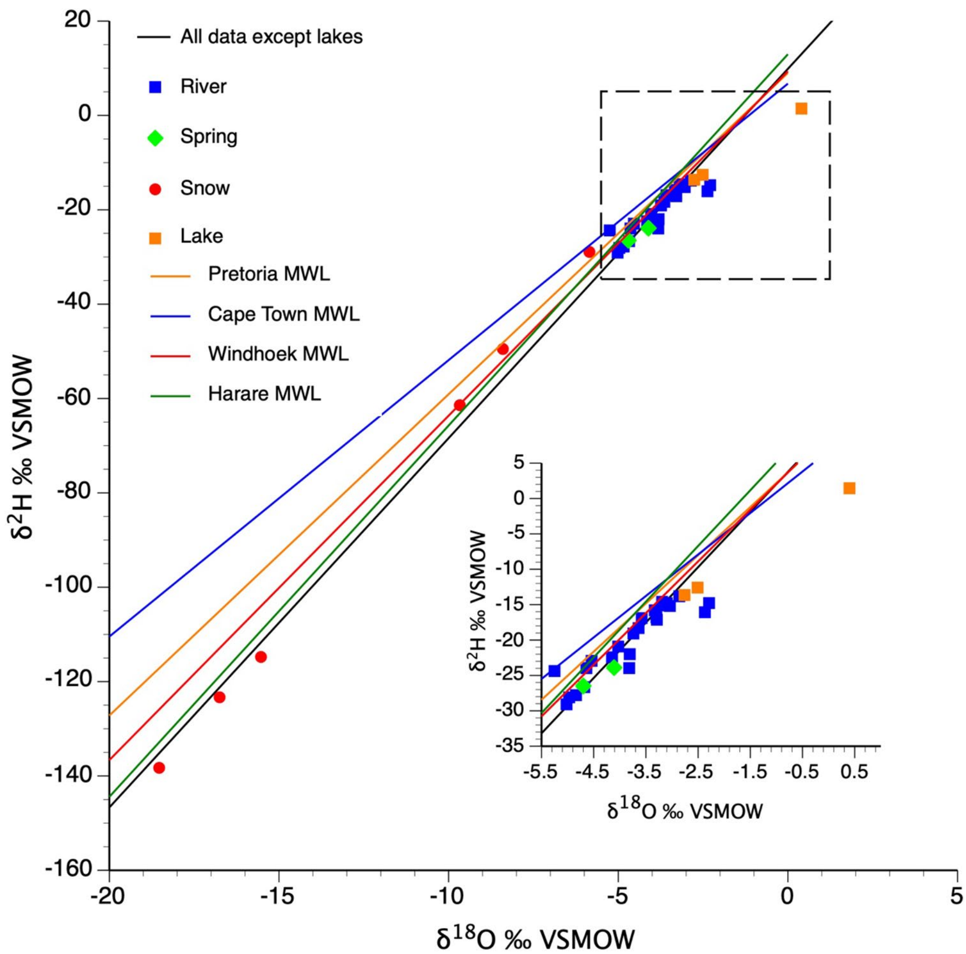

Fig. 2 $\delta^{18}O$ (**A** and **B**) and $\delta^{2}H$ (**C** and **D**) versus altitude and latitude for river samples only

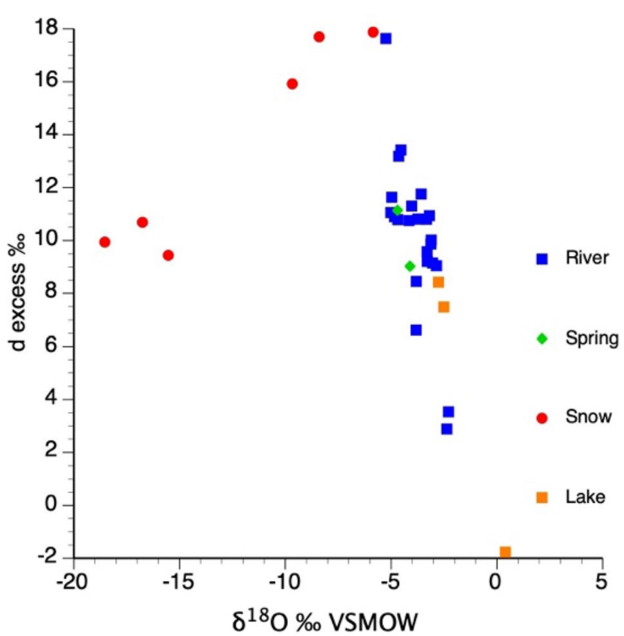

Fig. 3 Deuterium excess (d-excess) values versus $\delta^{18}O$ for all water samples

Windhoek MWL, rather than the Cape Town MWL. The isotopic composition of the spring samples from Lesotho is consistent with that of streams, although since only two springs were sampled, we cannot draw further conclusions based on spring composition.

4.2 Moisture source and air transport modelling

Averaging the 72-hour back trajectories of all air parcels for the 70 precipitation days, 11 dominant air parcel transport pathways are evident. Approximately 13.5% of the airmasses originate from south of the southern African subcontinent, tracking east and then north over the Indian Ocean, before recurving west to Lesotho (Fig. 5a). A further 12.9% originate further north over the Indian Ocean in the Mozambique Channel, curving northwest, before recurving south to Lesotho. The largest proportion of tracks, at 19.6%, originate over central Mozambique, and move west through southern Zimbabwe before recurving southwards to Lesotho. This dominant pathway is consistent with the alignment in the isotope records with the MWL for Harare. A similar anticlockwise track path is followed by air parcels

Table 4 Correlations between stable isotope ratios for river samples and geographical variables. * indicates statistically significant correlations

	Latitude	Longitude	Site Altitude	Source Altitude
$\delta^{18}O$	r = 0.08, p = 0.7102	r = – 0.40, p = 0.0528	*r = – 0.63, p = 0.0001	*r = – 0.62, p = 0.0012
$\delta^{2}H$	r = 0.27, p = 0.2020	*r = – 0.62, p = 0.0012	*r = – 0.71, p = 0.0001	*r = – 0.70, p = 0.0001
d-xs	r = 0.27, p = 0.2020	r = – 0.12, p = 0.5765	r = 0.24, p = 0.2586	r = 0.25, p = 0.2387

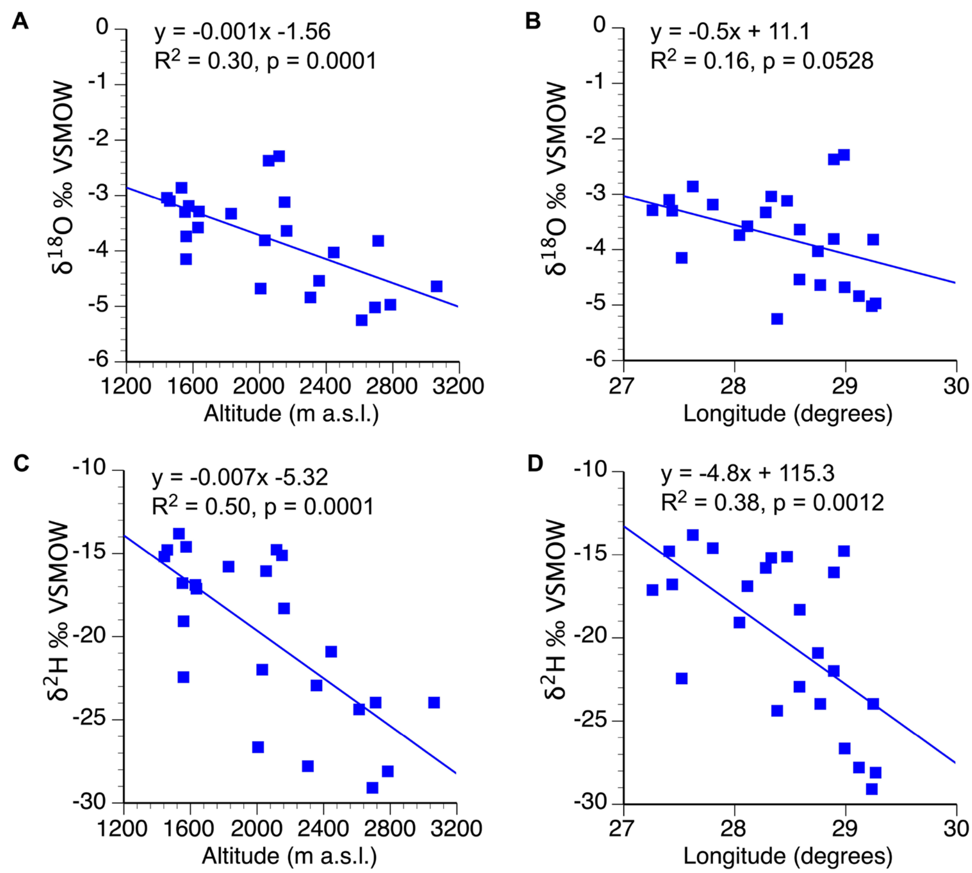

Fig. 4 $\delta^{18}O$ v $\delta^{2}H$ for A. The entire set of water and snowpack samples and B for all samples excluding snowpack. The regression line for this study describes all data except samples from lakes. Local meteoric water lines from the four southern African GNIP stations are also shown. For explanation, see text

originating over southeastern Botswana, tracking across Botswana (6.9%); central south Botswana, tracking due south to Lesotho (9.6%); western Botswana, tracking south along the Botswana-Namibia border (4.8%); and central Namibia, tracking southeast to Lesotho (4.1%). The latter two correspond with the alignment of the isotope values with the MWL for Windhoek. Approximately 17.7% of the tracks originate over the Atlantic Ocean and follow a due-easterly path to Lesotho. A further 2.7% originate south of southern Africa, tracking west before recurving north and then east over the Atlantic Ocean. A small proportion of tracks are very short in length, originating over land in close proximity to Lesotho from the south (2.0%), and north (6.2%) respectively (Fig. 5a).

Inspecting the individual 72-hour back-trajectories of all air masses for each storm event, there are no notable differences between the tracks, and in turn the broad climate dynamics, of snow and rain events collectively, nor any distinct shifts in the different types of tracks between seasons. There are, however, more frequent due-east tracks off the Atlantic Ocean during the winter months, and more common anticyclonic tracks off the Indian Ocean during the summer months. It is important to note that these refer to all air parcel trajectories, not all of which would be moisture bearing, or indeed sufficiently moisture bearing to contribute to a precipitation event along their trajectory or in the region of interest, Lesotho (Rapolaki et al. 2020). Exploring only those air masses that are close to (> 70% relative humidity) or at saturation (100% relative humidity), there are broad similarities in the distribution of clustered air masses (Fig. 5b). Following the work of Li et al. (2022a) in an alpine setting, we argue that an analysis of all air masses is likely to provide a more comprehensive overview of both the synoptic climate systems responsible for precipitation events, and of the pathways of moisture transport. This is because the rugged topography induces orographic saturation over

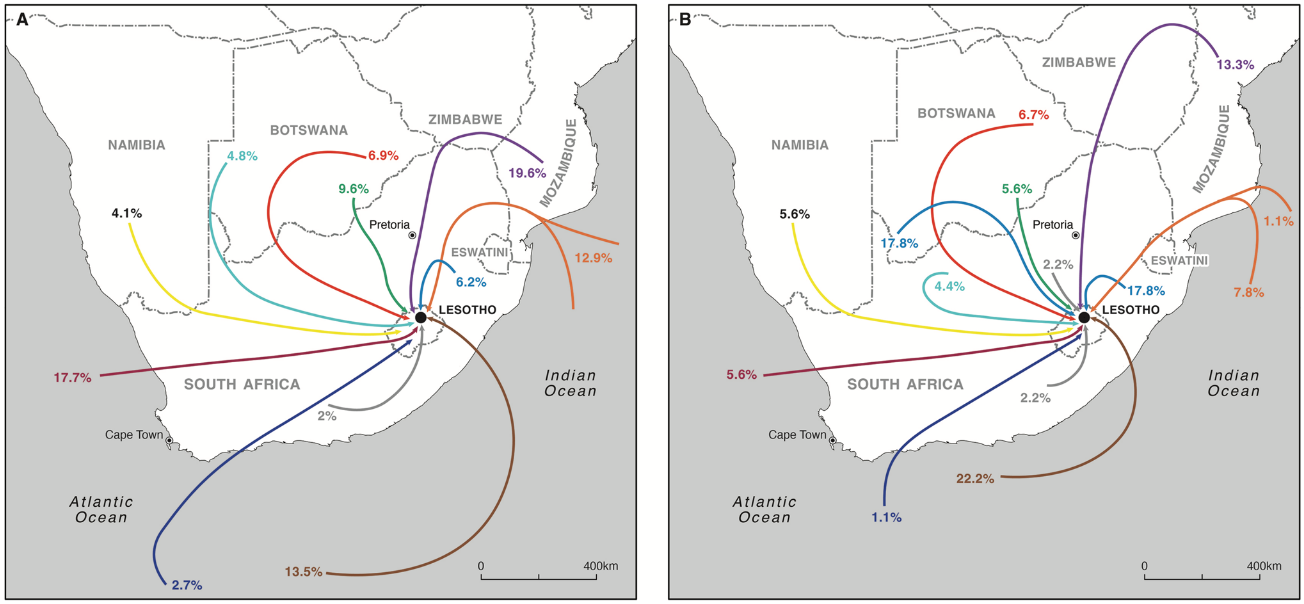

Fig. 5 **A** all proportional airmass trajectories, and **B** all saturated airmass trajectories, for Lesotho for each precipitation event over the period 30 May 2021–1 June 2022, modelled using HYSPLIT

much shorter timescales than the 6-hourly trajectories, and air masses that are at comparatively low relative humidity along their track to Lesotho may reach saturation due to the considerable uplift. This is demonstrated in particular by the precipitation events in Lesotho for which none of the air mass back trajectories have a modelled relative humidity of $>50\%$ for the 72-hour period prior to precipitation.

4.3 Spatial variations in surface-water isotope composition

The stable isotope values from the sampled surface water and snowpack in Lesotho demonstrate considerable spatial variation. The greatest variation is between the snow and water samples, as snow forms in clouds under non-equilibrium conditions (Lamb et al. 2017; Bagheri et al. 2019). Moreover, snow typically forms at low temperature and is thus heavy-isotope depleted in contrast to river waters, which tend to approximate the isotopic composition of weighted annual precipitation. There is notably less variation between the river, spring and dam samples than has been found elsewhere in southern Africa (Geppert et al. 2022). Despite the small number of samples, the dam waters may lie on a line with lower gradient than the rivers (Fig. 4), which is consistent with evaporative enrichment, commonly seen in lakes. The spatial variability in stable isotope values is consistent with the spatial heterogeneity in surface moisture and precipitation across Lesotho (Armstrong et al. 1993), a result of the rugged topography, particularly in the eastern Highlands (Sene et al. 1998). The negative correlation between both $\delta^{18}O$ and $\delta^{2}H$ and altitude (Fig. 2) is an expression of the well-known altitude effect, which arises from heavy-isotope depletion as air is forced to rise by the topography, leading to adiabatic cooling. The relationship with longitude, which is similar to that for altitude (although only statistically significant for $\delta^{2}H$) (Fig. 2), is also a reflection of the altitude effect, because the topography rises from west to east. These relationships are stronger than those found for Costa Rican surface waters (Lachniet and Patterson 2002) in a similar topopgraphic setting, where the strongest relationship was found between $\delta^{18}O$ values and altitude ($r=0.38$). Lachniet and Patterson (2002) interpret the weak correlations found in their study to represent complex and multi-variate influences of geographical variables. In the case of Lesotho, there likely are multivariate influences, and these statistically significant relationships for altitude and longitude do not preclude this. Moreover, as the difference in isotopic values between the Highlands and Lowlands (as defined by a 2000 m.asl threshold altitude) is weak but statistically significant, it is also likely that the relationships are not linear. Thus, while linear statistical tests have been employed in the interests of comparability of data, future analysis should explore more complex statistical models.

Deuterium excess in the Lesotho surface waters is likely to be strongly related to the d-excess in precipitation, which itself is controlled by conditions at the source of vapour formation (sea-surface temperature and, especially, relative humidity: Pfahl and Sodemann 2014) and modifications during vapour transport (Fröhlich et al. 2002). Given that the surface waters in our samples from Lesotho reflect the averages of moisture from several different sources, variations in source are unlikely to explain the range of d-excess values in Fig. 3. Instead, the negative correlation between $\delta^{18}O$ and d excess may be explained by enhanced evaporative loss of raindrops at higher temperature (higher $\delta^{18}O$ values) possibly associated with lower relative humidity. Possible evaporative enrichment of dam (lake) samples seems not to have modified these, so that they fall within the general trend of the surface waters. The snow samples, by contrast, show a positive correlation between $\delta^{18}O$ and d-excess. As noted, the snow packs samples accumulated during a single event and the variations may simply reflect variations in atmospheric temperature during that event.

The working understanding of the hydroclimate dynamics of Lesotho has been that the summer precipitation derives predominantly from the Indian Ocean, transported by the easterlies, and frequently takes the form of convective storms (Sene et al. 1998; Hydén 2002). Winter precipitation, often in the form of snowfalls in the eastern Lesotho Highlands, is understood to be associated with mid-latitude cyclones and associated CoLs, originating from the Southern Ocean and South Atlantic (Nel and Sumner 2008; Mulder and Grab 2009). On the basis of the dichotomy between easterly-derived summer precipitation, and westerly-derived winter precipitation, and of proximity to the sites, it was hypothesised that the meteoric water line for the Lesotho surface water samples would sit between that of Pretoria, representing the southern African easterly-derived summer-rainfall zone, and Cape Town, representing the westerly-derived winter rainfall zone, with a likely closer affinity to that of Pretoria. The results demonstrate a meteoric water line and d-excess that is most similar to that of the Harare GNIP station, and with greater similarity to the Windhoek station than to Pretoria or Cape Town, indicative of a primary moisture source north of South Africa. This is important when considering the impact that the progressive southward displacement of the westerlies (Sousa et al. 2018) may have on precipitation and water security in Lesotho in the future.

The role of TTT cloud bands, stretching from Namibia through to the southeast coast of South Africa, in inducing rainfall in subtropical southern Africa during summer months, is increasingly well understood as a synoptic phenomenon (e.g. Vigaud et al. 2012; Ratna et al. 2013; James et al. 2020). Moreover, the role of the TTTs in explaining convective rainfall in Lesotho has been documented (Crétat et al. 2012; Hart et al. 2013), but little interpretation has been conducted on the dynamics of this feature across the country. The TTTs and the South Indian Ocean Convergence Zone (SICZ) interact with a range of synoptic features including the Mascarene and St Helena Highs, the Angolan Low, the Congo Air Boundary, and the westerly storm tracks (James et al. 2020). Notably, a greater number of TTTs occur during La Niña years (Ratna et al. 2013);the year prior to sampling, which arguably represents the reservoir period for the surface water samples, followed a strong 'triple' La Niña (Jones 2022; Li et al. 2022b). Three dominant moisture sources have been identified for TTTs, namely a northerly flux from the Indian Ocean, a northwesterly flux from equatorial southern Africa and the far eastern equatorial Atlantic, and a southerly cyclonic flow around the TTT (Todd and Washington 1999: 941). These three fluxes align relatively well with the outputs of the HYSPLIT back-trajectory modelling for precipitation days in Lesotho. The dominance of the anticyclonic circulation track, which originates within the 72-hour window over the northeastern interior, likely originally from the Indian Ocean, and tracks through Zimbabwe, explains the strong coherence with the meteoric water line for Harare. Likewise, circulation through the TTT of moisture from the Atlantic Ocean would explain the similarities with Windhoek. The advection of air parcels in a south-easterly direction, along the SICZ, has been referred to in the case of smoke transport as the "river of smoke" (Swap et al. 2003: 1), and air-parcel trajectory analyses of air pollutants is consistent with those modelled for this study (Zunckel et al. 2000; Diab et al. 2004; Rose et al. 2020; Kok et al. 2021). To the best of our knowledge however, moisture transport along this "river of smoke" has not been explored in detail.

As there is no GNIP station, nor known rainfall isotope records, for Durban or similar sites along the east coast of southern Africa, it was not possible to identify a direct Indian Ocean rainfall isotope signal. This forms an important direction both for future research on surface water and rainfall isotopes in South Africa and Lesotho, and for higher resolution rainfall isotope data collection through GNIP. It will also be valuable to establish regular rainfall isotope monitoring within Lesotho, to contribute to the relatively sparse network of GNIP stations across southern Africa. Further analyses of the isotope record to investigate the source water of moisture in Lesotho would also benefit from a more extensive sampling of surface waters across Lesotho, repeated across different seasons.

5 Conclusion

This study presents the first analysis of hydrogen and oxygen isotopes from surface waters in Lesotho. The analysis of these isotopes reveals considerable spatial variability, with strong correlations between the isotope values and the site and source altitude of the river samples. For $\delta^{2}H$ strong relationships are also found with longitude, which due to the position of Lesotho and the Great Escarpment of southern Africa, represents a proxy for distance from the Indian Ocean and is also related to altitude. The meteoric water line for the Lesotho samples aligns most closely with that of the isotope data from the Harare GNIP station. This can be explained through the back-trajectory analysis of air parcel movement for the 72-hours prior to each precipitation event over the year leading up to sampling, with the greatest proportion of air mass trajectories circulating in an anticyclonic motion over continental southern Africa, passing through Zimbabwe. The alignment with the meteoric water line for Windhoek is less clearly supported by the results from HYSPLIT, but likely relates to the role of the TTT cloud band, and moisture transport that may be associated with the "river of smoke". More detailed analyses of these isotope records would benefit from a higher resolution rainfall isotope network in southern Africa, and in Lesotho. More detailed sampling of surface waters in Lesotho should focus on investigating any seasonal variations. This work is of value in understanding the contemporary synoptic systems responsible for precipitation in Lesotho, which would inform climate modelling and hydroclimate projection efforts in determining the future water security of both Lesotho, and South Africa's economic hub.

Supplementary Information The online version contains supplementary material available at https://doi.org/10.1007/s00382-023-07073-2.

Acknowledgements We thank Dr Mauro Lourenco for assistance in obtaining data on rainfall days for Lesotho. We thanks Dr Anne-Lise Jourdan for assistance in the Bloomsbury Environmental Isotope Facility. Permission for this study was granted by the Lesotho Ministry for Tourism, Environment and Culture.

Author Contributions JMF, JAH and AWM conceptualized the study. All authors were involved in the fieldwork and data collection. JMF and JAH led the data analysis and the first draft of the manuscript. All authors were involved in the revisions of the manuscript, and read and approved the final manuscript.

Funding Open access funding provided by University of the Witwatersrand. This work was supported by funding from the WITS-UCL Strategic Partnership Seed Funding granted to JMF, JAH and AWM.

Data Availability All data produced in this study are available within the dataset and supplementary files.

Declarations

Conflict of Interest The authors have no relevant financial or non-financial interests to disclose.

References

Archer E, Engelbrecht F, Hänsler A, Landman W, Tadross M, Helmschrot J (2018) Seasonal prediction and regional climate projections for southern Africa. In: Revermann R, Krewenka KM, Schmiedel U, Olwoch JM, Helmschrot J, Jürgens N (eds) Climate change and adaptive land management in southern Africa – assessments, changes, challenges, and solutions. Klaus Hess Publishers, Gottingen, pp 14–21

Armstrong M, Chetboun G, Hubert P (1993) Kriging the rainfall in Lesotho. Geostat Tróia 92:661–672

Bagheri R, Bagheri F, Karami GH, Jafari H (2019) Chemo-isotopes (^{18}O & ^{2}H) signatures and HYSPLIT model application: clues to the atmospheric moisture and air mass origins. Atmos Environ 215:116892

Bates MF, Haacke WD (2003) The frogs of Lesotho. Navorsings Van die Nasionale Museum Bloemfontein 19(6):110–112

Braun K, Bar-Matthews M, Ayalon A, Zilberman T, Matthews A (2017) Rainfall isotopic variability at the intersection between winter and summer rainfall regimes in coastal South Africa (Mossel Bay, Western Cape Province). S Afr J Geol 120:323–340

Chatanga P, Ntuli V, Mugomeri E, Keketsi T, Chikowore NVT (2019) Situational analysis of physico-chemical, biochemical and microbiological quality of water along Mohokare River, Lesotho. Egypt J Aquc Res 45(1):45–51

Crétat J, Richard Y, Pohl B, Rouault M, Reason C, Fauchereau N (2012) Recurrent daily rainfall patterns over South Africa and associated dynamics during the core of the austral summer. Int J Climatol 32(2):261–273

Dansgaard W (1964) Stable isotopes in precipitation. Tellus 16:436–468

Dedekind Z (2015) Modelling cumulus convection over the eastern escarpment of South Africa. MSc Dissertation submitted to North-West University, Potchefstroom

de Wet RF, West AG, Harris C (2020) Seasonal variation in tap water δ2H and δ18O isotopes reveals two tap water worlds. Sci Rep 10:13544. https://doi.org/10.1038/s41598-020-70317-2

Diab RD, Thompson AM, Mari K, Ramsay L, Coetzee GJR (2004) Tropospheric ozone climatology over Irene, South Africa from 1990 to 1994 and 1998 to 2002. J Geophys Res 109:2004JD004793. https://doi.org/10.1029/2004JD004793

Dunnink JA, Curtis CJ, Beukes JP, Van Zyl PG, Swartz J (2016) The sensitivity of afromontane tarns in the Maloti-Drakensberg region of South Africa and Lesotho to acidic deposition. Afr J Aquc Sci 41(4):413–426

Durowoju OS, Odiyo JO, Ekosse GIE (2019) Determination of isotopic composition of rainwater to generate local meteoric water line in Thohoyandou, Limpopo Province, South Africa. Water SA. https://doi.org/10.4314/wsa.v45i2.04

Fitchett JM, Mackay AW, Grab SW, Bamford MK (2017) Holocene climatic variability indicated by a multi-proxy record from southern Africa's highest wetland. Holocene 27(5):638–650

Fröhlich K, Gibson JJ, Aggarwal P (2002) Deuterium excess in precipitation and its climatological significance. Study of environmental change using isotope techniques. C & S Papers Series 13/P. International Atomic Energy Agency, Vienna, pp 54–66

Funk C, Peterson P, Landsfeld M, Pedreros D, Verdin J, Shukla S, Husak G, Rowland J, Harrison L, Hoell A, Michaelson J (2015)

The climate hazards infrared precipitation with stations—a new environmental record for monitoring extremes. Sci Data 2:150066
Geppert M, Hartmann K, Kirchner S, Pfahl S, Struck U, Riedel F (2022) Precipitation over southern Africa: moisture sources and isotopic composition. J Geophys Res Atmos 127(21):e2022JD037005. https://doi.org/10.1029/2022JD037005
Good SP, Mallia DV, Lin JC, Bowen GJ (2014) Stable isotope analysis of precipitation samples obtained via crowdsourcing reveals the spatiotemporal evolution of superstorm sandy. PLoS ONE 9(3):e91117
Grab SW, Nash DJ (2010) Documentary evidence of climate variability during cold seasons in Lesotho, southern Africa, 1833–1900. Clim Dyn 34:473–499
Grab S, Linde J, De Lemos H (2017) Some attributes of snow occurrence and snowmelt/sublimation rates in the Lesotho Highlands: environmental implications. Water SA 43(2):333–342
Gwimbi P, Selimo MJ (2020) Heavy metal concentrations in sediments and Cyprinus carpio from Maqalika Reservoir–Maseru, Lesotho: an analysis of potential health risks to Fish consumers. Toxicol Rep 7:475–479
Harris C, Burgers C, Miller J, Rawoot F (2010) O- and H-isotope record of Cape Town rainfall from 1996 to 2008, and its application to recharge studies of Table Mountain groundwater, South Africa. S Afr J Geol 113:33–56
Hart NC, Reason CJ, Fauchereau N (2013) Cloud bands over southern Africa: seasonality, contribution to rainfall variability and modulation by the MJO. Clim Dyn 41(5):1199–1212
Hitchcock RK (2015) The Lesotho Highlands water project: dams, development, and the World Bank. Sociol Anthropol 3(10):526–538
Hydén L (2002) The influence on summer rainfall in the Lesotho Lowlands from Indian Ocean SSTs. Hydrol Res 33(4):305–318
Hydén L, Sekoli T (2000) Possibilities to forecast early summer rainfall in the Lesotho Lowlands from El-Niño/Southern Oscillation. Water SA 26(1):83–90
Intergovernmental Panel on Climate Change (2021) Climate Change 2021: the physical science basis. Working Group I contribution to the sixth assessment report of the intergovernmental panel on climate change. Cambridge University Press, Cambridge
James R, Hart NC, Munday C, Reason CJ, Washington R (2020) Coupled climate model simulation of tropical–extratropical cloud bands over southern Africa. J Clim 33(19):8579–8602
Jones N (2022) Rare 'triple'la niña climate event looks likely. Nature 607:21
Kaseke KF, Wang L, Wanke H, Turewicz V, Koeniger P (2016) An analysis of precipitation isotope distributions across Namibia using historical data. PLoS ONE 11(5):e0154598. https://doi.org/10.1371/journal.pone.0154598
Kaseke KF, Wang L, Wanke H, Tian C, Lanning M, Jiao W (2018) Precipitation origins and key drivers of precipitation isotope (18O, 2H, and 17O) compositions over Windhoek. J Geophys Res Atmos. https://doi.org/10.1029/2018JD028470
Knight J, Grab SW (2018) Drainage network morphometry and evolution in the eastern Lesotho highlands, southern Africa. Quat Int 470:4–17
Kok L, van Zyl PG, Beukes JP, Swartz JS, Burger RP, Ellis S, Josipovic M, Vakkari V, Laakso L, Kulmala M (2021) Chemical composition of rain at a regional site on the South African Highveld. Water SA 47(3):326–337
Kylander ME, Holm M, Fitchett J, Grab S, Martinez Cortizas A, Norström E, Bindler R (2021) Late glacial (17,060–13,400 cal yr BP) sedimentary and paleoenvironmental evolution of the Sekhokong Range (Drakensberg), southern Africa. PLoS ONE 16(3):e0246821
Lachniet MS, Patterson WP (2002) Stable isotope values of Costa Rican surface waters. J Hydrol 260(1–4):135–150
Lamb KD, Clouser BW, Bolot M, Sarkozy L, Ebert V (2017) Laboratory measurements of HDO/H2O isotopic fractionation during ice deposition in simulated cirrus clouds. PNAS 114:5612–5617
Leketa K, Abiye T (2020) Investigating stable isotope effects and moisture trajectories for rainfall events in Johannesburg, South Africa. Water SA 46(3):429–437
Li G, Zhang XP, Xu YP, Song S, Wang YF, Ji XM, Xiang J, Yang J (2016) Characteristics of stable isotopes in precipitation and their moisture sources in Mengzi region, Southern Yunnam. Environ Sci 37:313–1320
Li T, Rao H, Li Y, Tan T (2022) Identifying the moisture source of atmospheric precipitation in a typical alpine river watershed using stable H-O isotopes and HYSPLIT model. Arab J Geosci. https://doi.org/10.1007/s12517-022-09596-0
Li X, Hu ZZ, Tseng YH, Liu Y, Liang P (2022) A historical perspective of the La Niña event in 2020/2021. J Geophys Res Atmos 127(7):e2021JD035546
Manhique AJ, Reason CJC, Rydberg L, Fauchereau N (2011) ENSO and Indian Ocean sea surface temperatures and their relationships with tropical temperate troughs over Mozambique and the Southwest Indian Ocean. Int J Clim 31(1):1–13
Matete M, Hassan R (2006) Integrated ecological economics accounting approach to evaluation of inter-basin water transfers: an application to the Lesotho Highlands Water Project. Ecol Econ 60(1):246–259
Mbata JN (2001) Land use practices in Lesotho: implications for sustainability in agricultural production. J Sustain Agr 18(2–3):5–24
Mook WG (2006) Introduction to Isotope hydrology. Stable and radioactive isotopes of hydrogen oxygen and carbon. Taylor and Francis, Oxford
Morris C (2017) Historical vegetation-environment patterns for assessing the impact of climate change in the mountains of Lesotho. Afr J Range Sci 34(1):45–51
Mukwada G, Taylor SJ, Manatsa D, Mahasa P, Robinson G (2020) Combating food insecurity in a rapidly changing mountain climate environment: insights from Lesotho. Clim Change 163(2):989–1006
Mulder N, Grab SW (2009) Contemporary spatio-temporal patterns of snow cover over the Drakensberg. S Afr J Sci 105(5):228–233
Nel W, Sumner P (2008) Rainfall and temperature attributes on the Lesotho–Drakensberg escarpment edge, southern Africa. Geogr Ann A 90(1):97–108
Norström E, Bringensparr C, Fitchett JM, Grab SW, Rydberg J, Kylander M (2018) Late-holocene climate and vegetation dynamics in eastern Lesotho highlands. Holocene 28(9):1483–1494
Pfahl S, Sodemann H (2014) What controls deuterium excess in global precipitation? Clim Past 10:771–781
Pryor JW, Zhang Q, Arias ME (2022) Integrating climate change, hydrology, and water footprint to measure water scarcity in Lesotho, Africa. J Water Res Plan Man 148(1):05021025
Putteman J, Buis K, De Doncker L, De Sutter R, Meire D, Schepens B, Troch P, Verhoeven R (2011) Integrated water resources management in the Orange-Senqu-Fish Catchment. In: International conference on the status and future of the world's large rivers, Vienna, 11–14 April 2011
Rapolaki RS, Blamey RC, Hermes JC, Reason CJC (2020) Moisture sources associated with heavy rainfall over the Limpopo River Basin, southern Africa. Clim Dyn 55:1473–1487
Ratna SB, Behera S, Ratnam JV, Takahashi K, Yamagata T (2013) An index for tropical temperate troughs over southern Africa. Clim Dyn 41(2):421–441
Ren W, Yao T, Xie S, He Y (2017) Controls on the stable isotopes in precipitation and surface waters across the southeastern tibetan Plateau. J Hydrol 545:276–287

Roffe SJ, Steinkopf J, Fitchett JM (2022) South African winter rainfall zone shifts: a comparison of seasonality metrics for Cape Town from 1841–1899 and 1933–2020. Theor Appl Climatol 147(3–4):1229–1247

Rose NL, Milner AM, Fitchett JM, Langerman KE, Yang H, Turner SD, Jourdan AL, Shilland J, Martins CC, de Souza AC, Curtis CJ (2020) Natural archives of long-range transported contamination at the remote lake Letšeng-la Letsie, Maloti Mountains, Lesotho. Sci Total Environ 737:139642

Rozanski K, Araguás-Araguás L, Gonfiantini R (1993) Isotopic patterns in modern global precipitation. In: Swart PK, Lohmann KC, McKenzie J, Savin S (eds) Climate Change in Continental Isotopic Records. Geophysical Monograph, vol 78. American Geophysical Union, Washington, pp 1–36

Saarinen J, Fitchett J, Hoogendoorn G (2022) Climate change and tourism in southern Africa. Abingdon, Routledge

Sene KJ, Jones DA, Meigh JR, Farquharson FAK (1998) Rainfall and flow variations in the Lesotho Highlands. Int J Climatol 18(3):329–345

Sengupta S, Sakar A (2006) Stable isotope evidence of dual (Arabian Sea and Bay of Bengal) vapour sources in monsoonal precipitation over north India. Earth Planet Sci Lett 250:511–521

Soderberg K, Good SP, O'Connor M, Wang L, Ryan K, Caylor KK (2013) Using atmospheric trajectories to model the isotopic composition of rainfall in central Kenya. Ecosphere 4(3):33

Sousa PM, Blamey RC, Reason CJ, Ramos AM, Trigo RM (2018) The 'Day Zero'Cape town drought and the poleward migration of moisture corridors. Environ Res Lett 13(12):124025

Stander JH, Dyson L, Engelbrecht CJ (2016) A snow forecasting decision tree for significant snowfall over the interior of South Africa. S Afr J Sci 112(9–10):1–10

Stein AF, Draxler RR, Rolph GD, Stunder BJB, Cohen MD, Ngan F (2015) NOAA's HYSPLIT atmospheric transport and dispersion modeling system. BAMS 96(12):2059–2077

Swap RJ, Annegarn HJ, Suttles JT, King MD, Platnick S, Privette JL, Scholes RJ (2003) Africa burning: a thematic analysis of the southern African Regional Science Initiative (SAFARI 2000). J Geophys Res Atmos 108(D13):2003JD003747. https://doi.org/10.1029/2003JD003747

Tanner A, Tohlang S, Van Niekerk P (2009) An overview of the engineering components Lesotho highlands water project. Civ Eng 5:28–35

Todd M, Washington R (1999) Circulation anomalies associated with tropical-temperate troughs in southern Africa and the South West. Indian Ocean Clim Dyn 15(12):937–951

United Nations Environment Programme (UNEP) (2010) Africa water atlas. United Nations Environment Programme, Nairobi

Vigaud N, Pohl B, Crétat J (2012) Tropical-temperate interactions over southern Africa simulated by a regional climate model. Clim Dyn 39(12):2895–2916

Vinti C (2022) An evaluation of Lesotho's right to expropriate the water in the treaty on the Lesotho highlands water project in a conflict of uses. Obiter 43(1):79–103

Vystavna Y, Matiatos I, Wassenaar LI (2021) Temperature and precipitation effects on the isotopic composition of global precipitation reveal long-term climate dynamics. Sci Rep 11:18503

Water security perspective for the Gauteng City Region GCRO, Gauteng City Region Observatory (GCRO), Johannesburg (2019). https://cdn.gcro.ac.za/media/documents/GCR_Water_Security_Perspective_for_web_2019.pdf. Accessed 24 July 2023

Wunderle S, Gross T, Hüsler F (2016) Snow extent variability in Lesotho derived from MODIS data (2000–2014). Remote Sens 8(6):448

Xie LH, Wei GJ, Deng WF, Zhao XL (2011) Daily δ^{18}O and δD of precipitation from 2007 to 2009 in Guangzhou, South China: implications for changes of moisture sources. J Hydrol 400:477–489

Xulu NG, Chikoore H, Bopape MJM, Nethengwe NS (2020) Climatology of the Mascarene High and its influence on weather and climate over southern Africa. Climate 8(7):86

Zunckel M, Robertson L, Tyson PD, Rodhe H (2000) Modelled transport and deposition of sulphur over Southern Africa. Atmos Environ 34:2797–2808

Publisher's Note Springer Nature remains neutral with regard to jurisdictional claims in published maps and institutional affiliations.